Keywords: methanol, port fuel injection, spray, phase Doppler interferometry, medium speed engines.

Design and characterisation of a port fuel injector for high power medium speed engines

Dr. Marco Coppo[1], Dr. Marco Ferro[1], Dr. Claudio Negri[1], Dr.-Ing. Fabian Pinkert[2], Dr. Mathias Niendorf[3]

(1) OMT SpA, (2) FVTR GmbH, (3) University of Rostock

https://doi.org/10.18453/rosdok_id00004648

Abstract

The marine engine industry is betting heavily on the adoption of new fuels, such as methanol, to reach the decarbonisation targets recently made more ambitious by IMO. Direct injection of methanol is set to achieve the highest substitution rates, therefore minimising the amount of diesel needed to pilot the ignition of the main fuel and the associated emissions [1].

However, this requires the design of large and complex dual fuel injectors capable to integrate in the same package both the diesel (for pilot and full backup power) and the methanol injection stages, which, in turn, requires significant modifications to the cylinder head. Furthermore, the pressurisation of methanol to direct injection pressure levels (around 600-700 bar) requires costly equipment not currently available at scale nor fit for integration in the engine room. For all these reasons, direct injection of methanol is mostly planned for new engine designs.

On the other hand, if significant benefits in terms of reduction of utilisation of fossil fuels are to be reached quickly, port fuel injection of methanol at relatively low pressures (10-50 bar) promises to provide an easier, faster and more cost effective solution to convert the existing engine fleet.

The paper presents the port fuel injector developed by OMT to answer the need of powering large medium speed engines with unit power up to 1200 kW/cylinder, and the challenges addressed during development. The main issue that such injection technology needs to address is to achieve a fine atomisation of the fuel, so that it can be transported by the charge air into the cylinder without wetting the intake manifold walls, without having the possibility to rely on a high supply pressure. Furthermore, direct actuation is required due to the need to avoid a methanol return line, posing challenges in terms of actuation forces, which should contrast the spring force needed to ensure proper sealing in between injections. These challenges are discussed in the paper and the technical solution identified to address them is presented.

The article also presents the test setup devised to measure the spray characteristics and discusses the results of a Phase Doppler Interferometry (PDI) experimental campaign aimed at measuring spray parameters at different distances from the injector tip. Water spray data is provided in the present paper, and further tests are planned to characterise also the methanol spray with the aim of defining a correlation that could simplify further tests by running them with water only.

1. Introduction

In July 2023 IMO raised the bar for the whole marine industry by revising its strategy on reduction of greenhouse gas (GHG) emissions from ships [2], which led to the definition of more ambitious targets aimed at reaching net-zero emissions by 2050. Considering the typical vessel lifespan of 30 years, it follows that the global fleet that will have to achieve this target will largely consist of vessels built already in the next decade. This consideration forced ship owners to think carefully about their next investments, and resulted in an increased pressure on vessel and engine designers to provide, in the shortest possible time, commercially-ready solutions able to operate with synthetic renewable fuels such as methanol and ammonia [3].

However, in the same strategic document, IMO also set GHG reduction targets for 2030 (-30%) and 2040 (-80%), which are, in perspective, even more challenging to achieve as they can only be reached through a significant retrofitting of the existing fleet of vessels because the relative impact of newbuilds will be initially limited. It follows that the industry must support this additional market demand by providing cost effective and simple retrofit kits to rapidly scale up conversion projects, even if at the partial expense of maximum efficiency and GHG emission reduction.

According to [4], methanol obtained from renewable sources will be available sooner than ammonia and, in perspective, prices of the two fuels in the future will be comparable. Furthermore, methanol toxicity is lower than that of ammonia. This, coupled with the fact that it is easier to handle because it can be stored in liquid state at ambient pressure, makes methanol the current fuel choice for conversion projects.

Both lean-burn premixed combustion and diffusive combustion of methanol are technically possible. In the former, liquid fuel is introduced in the intake manifold through one or more port fuel injectors operating at fairly low pressure (10-30 bar) which are tasked with the atomization of the liquid jet so that the resulting droplets can be mixed with and transported by the air flow into the combustion chamber during the intake stroke. The air/fuel mixture is then ignited through a pilot injection of diesel fuel delivered by the standard injector used also for full diesel operation when methanol is not available.

On the other hand, direct injection of methanol in the combustion chamber requires the integration on the cylinder heads of dedicated injectors operating at high pressure (typically 600 800 bar), and the installation of an expensive pumping system to pressurize the fuel. As the space on the cylinder head is already limited, the integration of diesel and methanol injectors into one object is very challenging and leads to custom-made and fairly expensive solutions.

As reported in detail in [1] and [6], the direct injection technology is advantageous in terms of higher engine efficiency and fuel substitution ratio (i.e. smaller pilot injection quantities are required to ensure stable methanol combustion), when compared to port fuel injection. Additionally, the diffusive combustion approach limits the contact of unburnt fuel with cylinder liner walls, reducing issues related to engine oil contamination and piston/liner scuffing due to oil film breakup.
Conversely, a port fuel injection system is simpler in terms of number and complexity of components and in terms of installation constraints, which makes it cheaper than a direct injection one, and thus ideally suited to retrofitting existing diesel engines. In order to support its customers on their path to decarbonization, OMT developed a methanol port fuel injector suitable to power the largest medium speed marine engines. The paper presents the challenges faced during design and how they were

addressed, as well as reporting injector performance data both in terms of dynamics and of spray quality.

2. OMT Methanol Port Fuel Injector

2.1. Injector architecture

The injector is designed for a multi-point injection layout, i.e. with one injector for each cylinder, and for an engine power up to 1200 kW/cylinder. It is able to deliver the rated injected quantity of 29000 mm³/shot in 80° CA for an engine speed of 500 rpm with a methanol supply pressure of 30 bar. A section view of the injector and of its main component is shown in Figure 1. To limit the complexity of the engine interface, the injector is directly actuated by a solenoid, so that fuel return or control oil feeding and return lines are not needed. All potential leakages are directed towards a dedicated line with a low positive pressure of nitrogen or in vacuum, to avoid the possibility of formation of an explosive mixture, making the injector ATEX compliant. Finally, an inbuilt flow fuse limits the injected quantity in case of malfunctioning.
To maximize the atomization of the fuel with the limited differential pressure available, an outward-opening poppet valve architecture was chosen: given the same fluid characteristics, injection pressure and downstream conditions, the size of the droplets is proportional to the characteristic dimension of the liquid jet forming at the nozzle outlet (see [7] and [8]). Although the injection duration is approximately three times larger than for the case of direct injection, due to the much lower supply pressure, a much larger fuel passage section is required. Therefore, for this particular application, an implementation similar to that of high-pressure injectors, i.e. with holes open in a sac downstream of the needle seat, would require a very high number of holes to obtain a comparable thickness of the liquid film of the one that can be created at the exit of a poppet valve. As shown in Figure 2, thanks to a particularly narrow and long exit section of the poppet, it is possible to generate a liquid film with a thickness of less than 0.6 mm, which, in turn, is able to generate a spray with very fine droplets. Moreover, for this layout almost all the pressure available is used to generate fluid velocity, while in a traditional architecture some pressure is lost at the needle seat, especially considering that the maximum stroke of the needle is limited by the magnetic force available at the solenoid. Another advantage of the outward opening architecture is that it is possible to balance the fuel pressure forces on the needle, so that the actuator needs to counteract spring and inertia forces only, limiting the size and cost of the solenoid and, consequently, those of the injector. Moreover, in this configuration the intake manifold pressure acts in the direction of closing the needle, increasing the force on the seat and providing additional robustness against injector leakage.

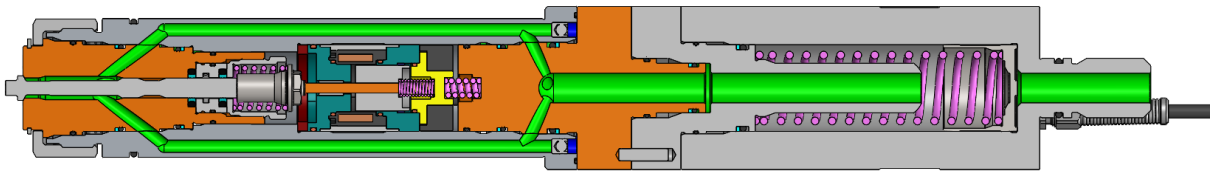

Figure 1: OMT PFI injector

A possible drawback of this architecture is that it is not possible to orient the spray with respect to the injector axis. However, the spray cone angle was chosen to be large enough (120°) to minimize

the risk of fuel impacting the manifold walls. By mounting the injector with its axis almost perpendicular to that of the intake manifold, the relative velocity of the spray with respect to the charge air flow is maximised for the portion of the spray propagating upstream in the intake manifold, consequently increasing the atomization of the droplets, while for the remaining part of the spray the droplets can proceed along the manifold for a long path and have therefore enough time to evaporate before encountering obstacles.

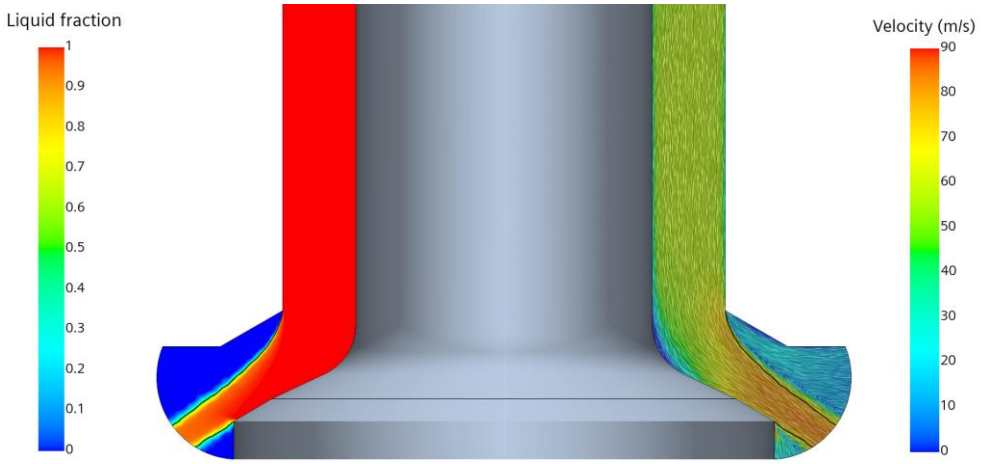

Figure 2: CFD simulation of the fuel motion at the injector exit in still air. Velocity field (right) and liquid fraction (left)

2.2. Injector Performance

A dedicated test bench (see Figure 3) was especially designed and procured to test and validate the PFI injectors. It allows injection of test oil or distilled water into a chamber filled with air at a configurable pressure, to simulate the actual injection condition of the engine intake manifold. Water temperature can be controlled up to 70 °C, to achieve conditions of similarity with methanol in terms of dynamic viscosity and vapour pressure, and hence properly validate injector operation in similar conditions of lubrication of the sliding components and cavitation onset as those in the field. Optical access to the spray chamber is allowed through a glass panel, so that investigation on the spray formation and evolution can be conducted in-house. The measurement is fully automated and it allows the acquisition of the mean injected mass and of the instantaneous needle lift, from which the injection rate shape of each shot can be reconstructed, allowing for the determination of the shot-to-shot dispersion of the injector.

Figure 3: PFI injector test bench (left), detailed view of the injection chamber (right)

Figure 4 and Figure 5 show a comparison between experimental results and data obtained from a lumped parameter simulation of the injector, performed with GT-Suite. Given the quite low operating pressure range, the behaviour of the injector is significantly affected by the geometrical characteristics of the upstream feeding line, hence they were considered and included into the model. It can be observed that very good agreement between simulated and tested injector lift is obtained both for a rated injection (see Figure 4) and for a smaller injection quantity (see Figure 5). Moreover, it can be observed that a small part-to-part variation of injection performance was obtained, with a dispersion for a rated injection limited to ±2% of injected mass.

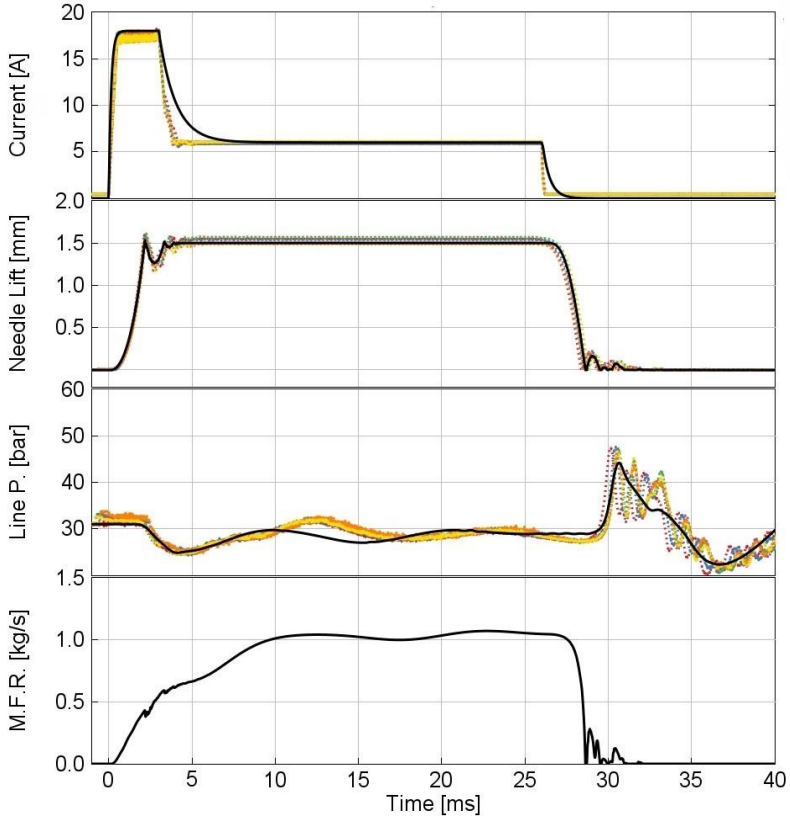

Figure 4: Comparison of simulation data (black solid line) with experimental results of 6 different injectors (dotted colored lines) for a rated injection

Once the lumped-parameter model is validated, it is possible to perform a simulation of the injector performance on the engine, to account for the actual geometry of the feeding line. Figure 6 shows a comparison between simulated injector operation on the test-bench and in the engine layout. It can be noticed how the difference in the pressure fluctuations in the upstream line considerably affects the injection rate shape and the total injected mass, highlighting the need for a differentiation of these two operation conditions when validating experimental data.

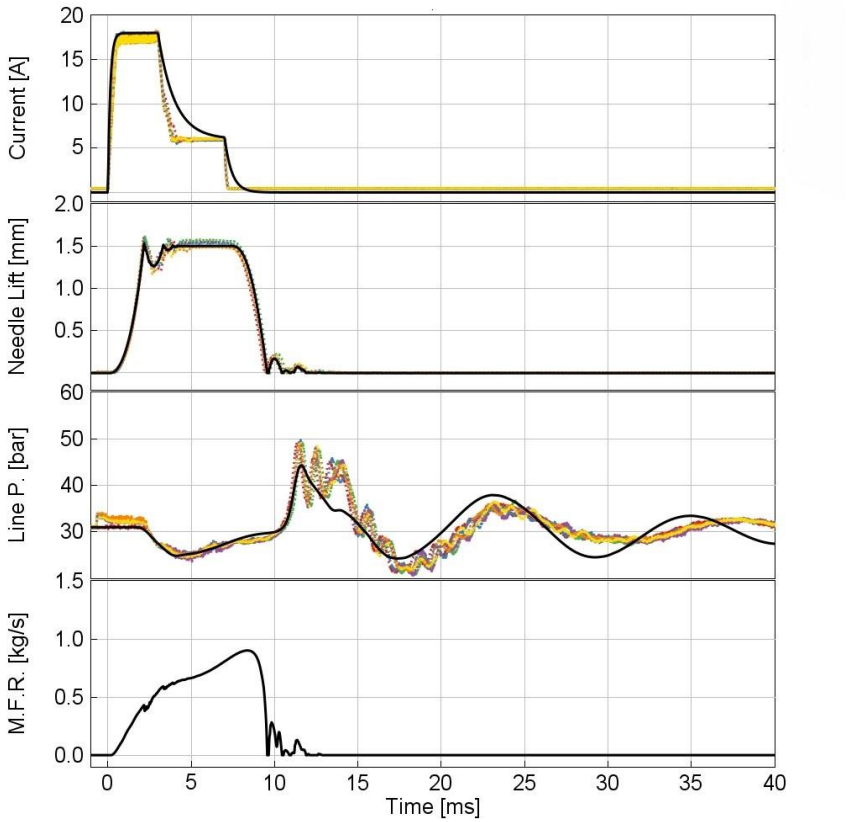

Figure 5: Comparison of simulation data (black line) with experimental results of 6 different injectors (dotted colored lines) for an injection equal to 30% of the rated injection

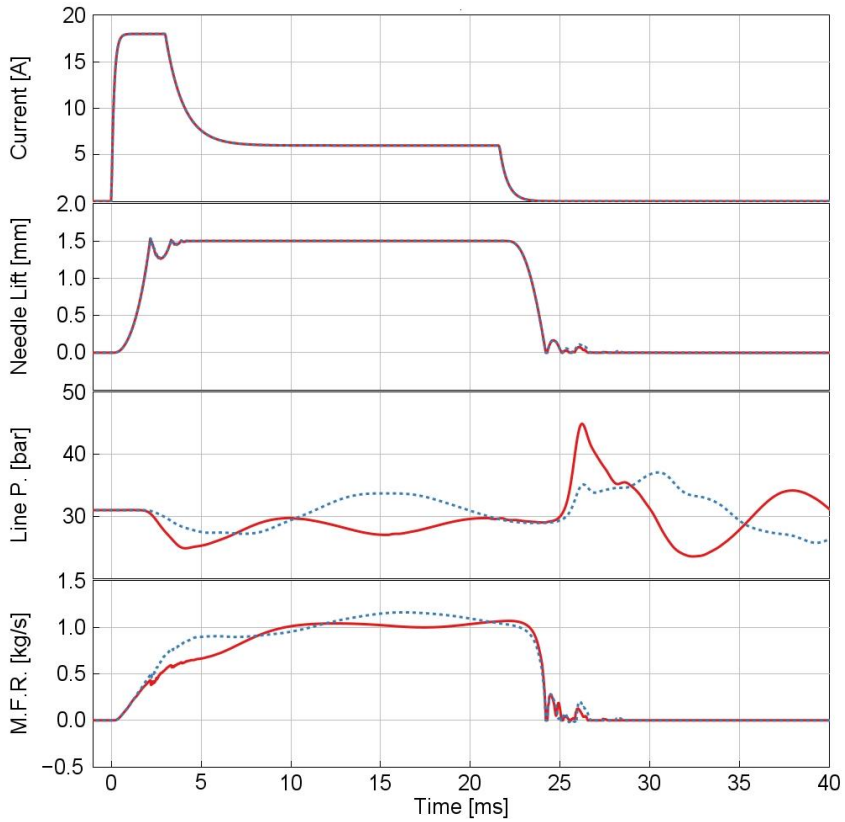

Figure 6: Simulation results considering the upstream feeding line of the test bench (solid line) vs. the actual engine layout (blue dotted line)

3. Spray Analysis

3.1. Experimental Setup and measurement procedures

The injector was tested in a newly developed test bench, designed for droplet sizing and spray visualization of methanol sprays. The sprays can be measured in quiescent air at ambient pressure and temperature. The test cell shown in figure 7 consists of a stainless-steel tank, fitted with multiple windows for the Phase Doppler Interferometry (PDI) system and for the high-speed camera. While the measurement system is fixed in space, the injector is positioned by a 2-axis traverse, allowing measurements from 120 to 370 mm nozzle distance.

Methanol or water is pressurized by an air-driven piston pump, allowing injection pressures of up to 1000 bar. In this test setup with injection pressures up to 25 bar the fluid is stored in a pneumatic accumulator close to the injector with a volume of 0,46 liters. A high-speed pressure transducer, mounted between the injector and the accumulator, shows the effectiveness of the accumulator in limiting the pressure loss during the injection to 11%.

After injection, the water or methanol mist is roughly separated from the scavenging air and then filtered using active carbon filters. The air scavenging flow in the test chamber is provided by a side channel blower situated behind the chamber. The test chamber pressure is kept very slightly below the atmospheric level as a part of the safety concept for confining the methanol vapors. The inside of the chamber is an explosion prevention zone.

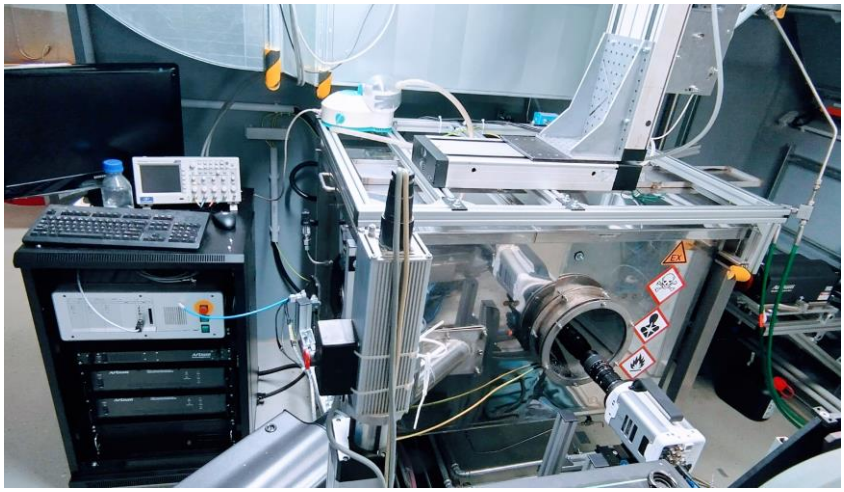

Figure 7: Particle Distribution and Spray test bench for analyzing methanol sprays

The droplet size measurements were carried out using an Artium Phase Doppler Interferometer. This system allows the measurement of velocity and diameter of droplets passing through the measurement volume. This volume of about 1mm³ is formed by the intersection of two laser beams. Droplets passing the measurement volume refract the fringe pattern of the laser beams into an array of three optical receivers. From the frequency of the signal and phase shift between the receivers, the velocity and diameter of the droplets can be calculated. [10]

The system was operated using two optical setups and, initially, operating the injector with water at room temperature. A receiver focal length of 1000 mm was found to disregard droplets above 500 µm. As larger droplets are believed to be important in the practical application of the spray within the intake manifold, a second focal length of 2000 mm was employed to capture droplets up to 1000 µm. Comparing the results obtained with the two measurement configurations, it was found that the second setup disregards droplets below 80 µm. The resulting droplet distribution histograms obtained with the two setups are compared in Figure 8 for one operating point, and the filtering effects at both ends of the particle diameter range are clearly visible. The results of both setups were combined with an overlap of the distributions between 100 and 300 µm to yield the most accurate results. In this way, the resulting measurable droplet range was between 40 and 1000 µm.

Finally, to gain a basic understanding of the spatial location and temporal evolution of the spray, high speed videos were captured of the entire spray cone and of the near nozzle region. For these measurements, a Photron Nova camera was used. The spray was illuminated from two sides by xenon light flashes.

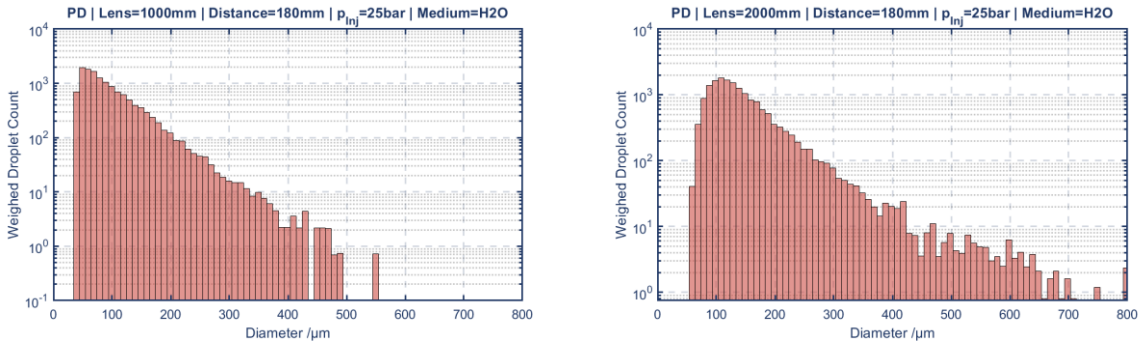

Figure 8: Comparison of the probability distribution (PD) histograms for two PDI Setups. The 1000 mm lens was found to disregard droplets above 500 µm while the 2000 mm lens was found to disregard droplets below 80 µm

3.2. Measurements results

The temporal evolution of the sprays in Figure 9 shows an opening phase of the needle between 1 and 3 ms after start of energization. In this phase a dominating instability frequency of the liquid sheet can be observed. At full needle lift water is injected with visibly stronger perturbations leading to a finer primary breakup. The cone half angle in the near nozzle region was measured to be 56,5°.

The PDI measurements were performed at injection pressures of 10 bar and 25 bar, to match the pressure differential of 15 and 30 bar injection pressure and 5 bar counter pressure in the intake manifold. The measurement locations were set in polar coordinates as the distance from the nozzle and the cone half angle. The nozzle distances chosen for this investigation were 180 and 340 mm. The spray was scanned in 1° intervals from 52° to 58° half cone angle. Most measurements were performed in the middle of the spray at about 55° to obtain a large data base for the probability distribution (PD) analysis. The average droplet diameters were calculated individually for all spray positions and averaged with weights corresponding to the total volume of liquid measured at each location.

The presented results are based on combined data from both focal lengths to provide good measurement accuracy at both ends of the size spectrum. Figure 10 visualizes the obtained particle distributions for all measurement locations across the spray in histograms. Three histograms appear to have an adequate resolution due to the large number of droplets measured. For the measurement point at 10 bar differential pressure and 340mm nozzle distance only a small number of droplet counts were obtained. It is likely that at this operating point the smallest droplets are underrepresented: the low spray velocity due to the low injection pressure combined with the large distance allows the smallest droplets to disperse over a large area and thus escape the measurement volume. For this reason, the results of this measurement point are not taken to be representative and are not further included in the comparison.

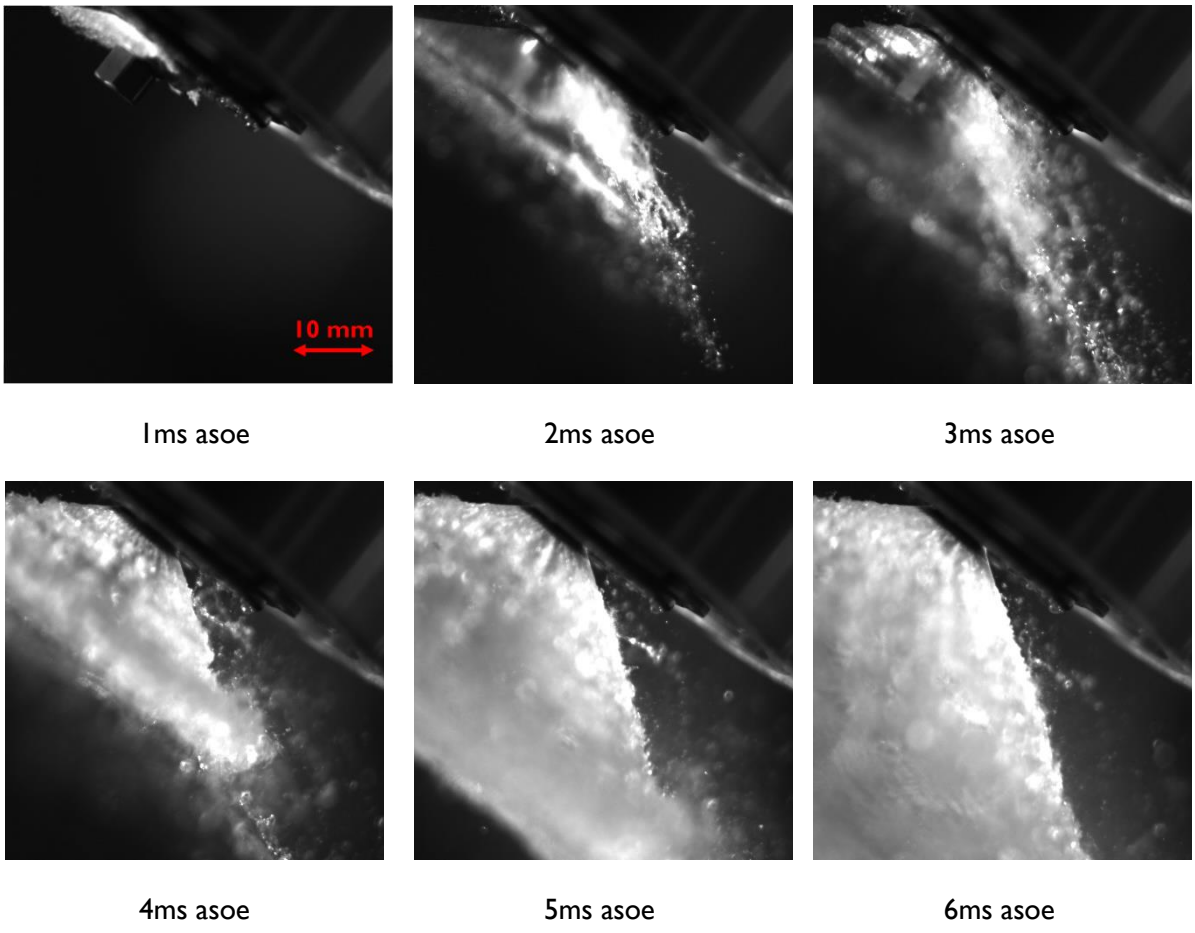

Figure 9: Spray evolution at 2 bar injection pressure in 1ms intervals after start of energization (asoe). Full lift of the poppet valve is reached after about 3 ms asoe. The measured cone half angle near the nozzle was 56,5°

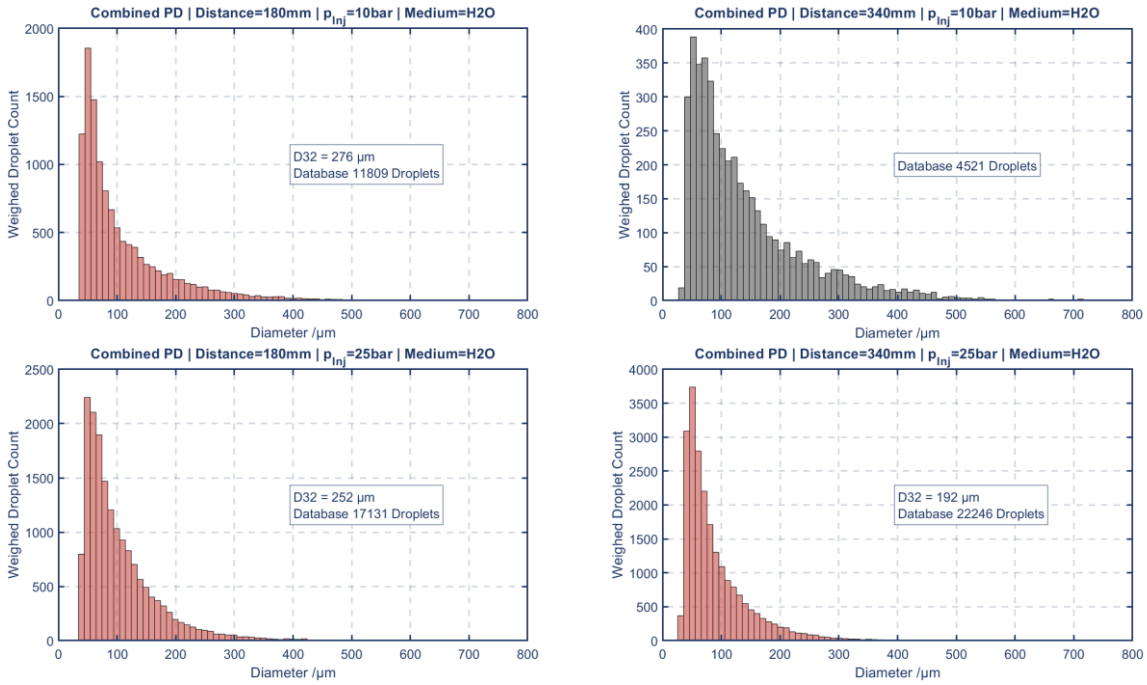

Figure 10: Particle Distributions at 180 and 340 mm distance from the nozzle at 10 and 25 bar injection pressure. A wider distribution at the low injection pressure can be observed. The histogram at 340 mm and 10 bar is believed to be unrepresentative of the spray because of the low number of droplets and the atypical histogram shape

A comparison of the mean diameters obtained is given in Figure 11. The Sauter mean diameter (SMD, D_{32}) was chosen as spray metrics, because of its extensive use in characterization of fuel sprays. For 25 bar of differential pressure, a distinct reduction in droplet diameter can be observed with further distance from the nozzle, and the SMD reaches a level of 192 µm at 340 mm from the nozzle. This can be explained by the droplet velocity: high droplet velocities lead to secondary breakup of larger droplets due to the aerodynamic forces. The driving non-dimensional parameter describing this instability is the Weber Number. As reported in [9], starting from a Weber number of about 12 bag breakup of droplets can occur, leading to a reduction of the mean diameter of a droplet ensemble.

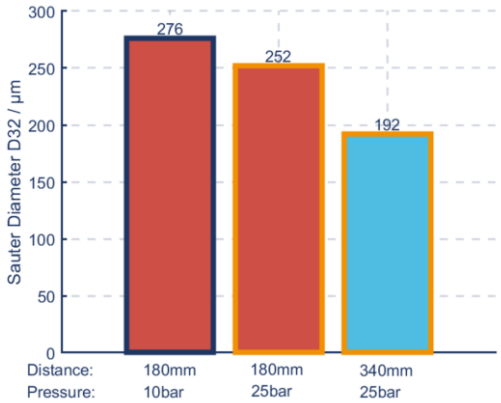

Figure 11: Resulting SMD for all operating points. The reduction of the diameter at 25 bar is likely due to secondary breakup.

To visualize the influence of the velocity on the evolution of the spray, 2D histograms of droplet diameter and velocity are shown in Figure 12. In the top row, at 10 bar injection differential pressure

the larger droplets have a velocity of up to 30 m/s and hardly any droplets have Weber Numbers above 12. On the contrary, as shown in the bottom left plot, at a differential pressure of 25 bar a significant number of droplets are in the region of secondary breakup. These break up and disappear going to 340mm distance (bottom right), thereby lowering the mean diameter. Furthermore, the whole of the ensemble gets slowed down. These findings not only serve to explain the experimental results but also give insight into the benefits of high injection velocities and into the effect of aerodynamic forces onto droplet distributions. Considering that in the intake manifold the air velocity reaches up to 100 m/s, we can expect that, given the larger relative velocity of the droplets in respect with the surrounding air flow, an even larger portion of droplets would undergo secondary breakup, thus lowering the effective mean diameter of the resulting spray. Moreover, the lower surface tension of methanol would increase even more the Weber number, further decreasing the SMD of the spray in real operating conditions.

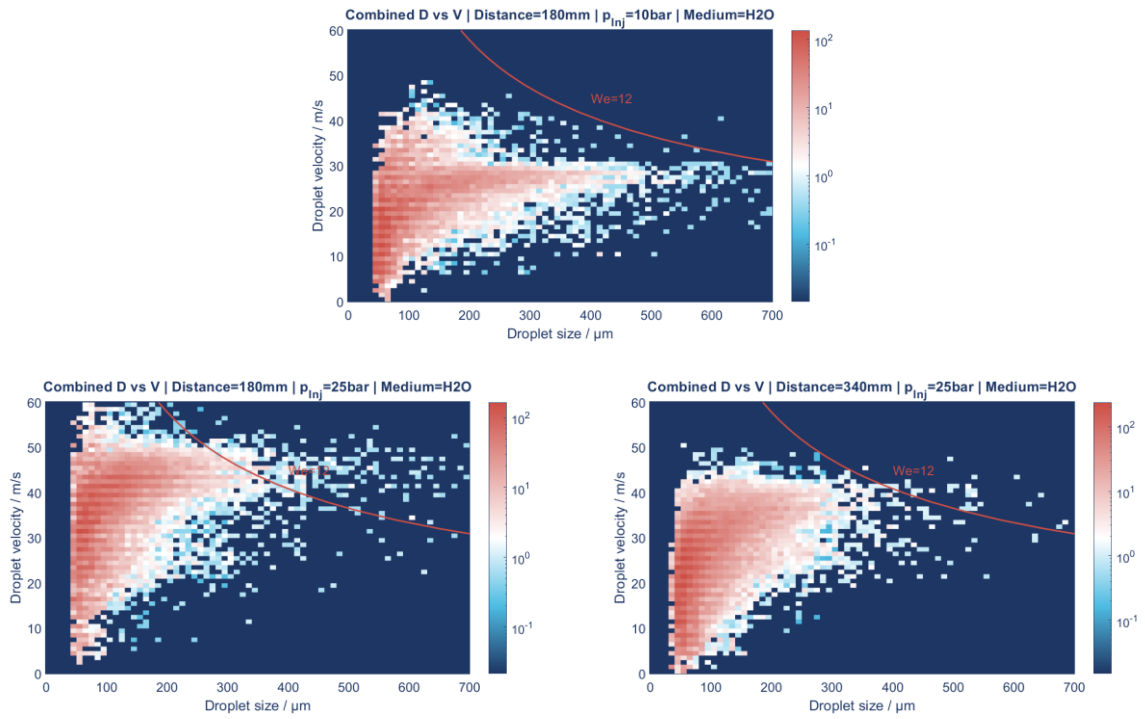

Figure 12: Two dimensional histograms of droplet velocity and droplet size for all operating points. The colormap is in logarithmic scale to allow visibility of the scarce occurrences of larger droplets. The critical Weber number of 12 is plotted in the diagrams to indicate regions of secondary breakup towards high diameters and high velocities.

4. Conclusions

In this paper the design of the OMT methanol port fuel injector for engines with power up to 1200 kW/cylinder has been presented and the main design choices illustrated. It was shown that, with an outward-opening poppet valve architecture, large volume flow rate can be achieved while keeping at a minimum the characteristic length scale of the injected fluid film, hence maximizing the quality of atomization. Measured injector performance matches well the simulated behaviour, and good injection repeatability was achieved.

To characterize the spray generated by the injector, a new test bench has been designed and built at FVTR, allowing to safely perform PDI and other measurements with low viscosity fuels such as

methanol. Measurement results showed that the OMT injector is capable of generating a fine spray, with a SMD of about 200 µm at a distance of 340 mm from the nozzle when water is used as fluid.

The next step is continuing the measurements across a larger number of operating points and locations, completing the characterization of the spray of the new injector and allowing to build a solid understanding of the atomization mechanism. Moreover, extending the measurement to the case of methanol injection will allow to understand the effect of the variation of fluid property on the spray particle distributions, to validate and tune existing correlation and scaling laws for this flow case, and to create a database for validating ongoing CFD simulations of the spray evolution.

Acknowledgments

The authors would like to acknowledge the colleagues at OMT their support in providing data and valuable input for writing this paper.

Literature

[1] Yin, X., et al., "In-depth comparison of methanol port and direct injection strategies in a methanol/diesel dual fuel engine", Fluid Processing Technology, Vol. 241, March 2023, 107607.

[2] International Maritime Organisation, "2023 IMO Strategy on Reduction of GHG Emissions from Ships", Resolution MEPC.377(80), 2023, London, United Kingdom.

[3] Coppo, M., et al., "Powering a greener future: the OMT injector enables high-pressure injection of ammonia and methanol", CIMAC Congress paper 139, 2023, Busan, South Korea.

[4] DNV, "Maritime Forecast to 2050 – Energy Transition Outlook 2023", 2023, Høvik, Norway.

[5] Dierickx, J. et al., "Retrofitting a high-speed marine engine to dual-fuel methanol-diesel operation: A comparison of multiple and single point methanol port injection", Fuel Communications, Vol. 7, June 2021, 100010.

[6] Altun, Ş. et al., "Comparison of direct and port injection of methanol in a RCCI engine using diesel and biodiesel as high reactivity fuels", Process Safety and Environmental Protection, Vol. 174, June 2023, pp. 681-693.

[7] Kooij S. et al. "What determines the drop size in sprays?" Physical review X, Vol. 8, July-September 2018, pp. 031019.

[8] Hiroyasu H. and Arai M. "Structures of Fuel Sprays in Diesel Engines." SAE Transactions, vol. 99, 1990, pp. 1050–61.

[9] Jain, Mohit, R. Surya Prakash, Gaurav Tomar, und R. V. Ravikrishna. "Secondary breakup of a drop at moderate Weber numbers". Proceedings of the Royal Society A: Mathematical, Physical and Engineering Sciences 471, Nr. 2177 (8. Mai 2015): 20140930.

[10] Ofner, B. (2001). Phase Doppler Anemometry (PDA). In: Mayinger, F., Feldmann, O. (eds) Optical Measurements. Heat and Mass Transfer. Springer, Berlin, Heidelberg.